Journal of Applied Polymer Science

Dissipative particle dynamics studies on the interfacial tension of A/B homopolymer blends and the effect of Janus nanorods

Chun Zhou ,[1,2] Shi-kai Luo,[1,2] Yi Sun,[1] Yang Zhou,[2] Wen Qian[2]

[1]School of Materials Science and Engineering, Southwest University of Science and Technology, Mianyang 621010, China
[2]Institute of Chemical Materials, Chinese Academy of Engineering and Physics, Mianyang 621900, China
Correspondence to: Y. Zhou (E-mail: youngzhou1980@126.com) and Y. Sun (E-mail: hmily-sunny@163.com)

ABSTRACT: Janus nanorods are used as a novel rigid compatibilizer to improve the interfacial tension of incompatible A/B homopolymer blends. Dissipative particle dynamics (DPD) methods are preformed to explore the effect of Janus nanorods on the interfacial tension. The results show that Janus nanorods are a good compatibilizer only when the appropriate length is chosen, which is different from the traditional coil compatibilizer (surfactants and block copolymers). The length of the Janus nanorods can significantly influence their orientation through the competition between the entropic and enthalpic effects. The shorter Janus nanorods preferring "standing" have a better efficiency in improving the interfacial tension than the longer ones preferring "lying." If we can control the orientation of the longer Janus nanorods, they are still a good compatibilizer. This simulation work can widen the application of Janus nanoparticles. © 2016 Wiley Periodicals, Inc. J. Appl. Polym. Sci. **2016**, *133*, 44098.

KEYWORDS: blends; compatibilization; nanoparticles; nanowires and nanocrystals; surfaces and interfaces; theory and modeling

Received 25 March 2016; accepted 19 June 2016
DOI: 10.1002/app.44098

INTRODUCTION

The properties of immiscible homopolymer blends are governed to a large extent by their interfacial characteristics.[1] Hence, it is crucial to finely control the interfaces to tailor the basic properties of these systems. As a conventional coil compatibilizer, amphiphilic surfactants and block copolymers [Figure 1(a,b)] were often added to the blends to achieve this aim.[2–8] Recently, rigid nanoparticles have often been utilized to control the polymer structures as a strategy for tailoring the properties of the material,[9–19] since the rigid nanoparticles can self-assemble at the interface of the two phases and influence the interfacial properties. For example, Luo and coworkers[12–15] investigated the effect of the nanoparticles on the water/trichloroethylene interface. Fan *et al.*[16] showed that the decane/water interfacial tension is not much influenced by the silica nanoparticles with different surface chemistry. Yan and coworkers[17–19] testified that the nanorod can decrease the interfacial tension. However, they did not provide the measurable relationships. Our work first showed the measurable scaling rules for homogenous nanorods [surface-modified by a single polymer, Figure 1(c)] and the interfacial properties (including the interfacial tension and thickness) of immiscible blends.[20] These works clarified an important viewpoint that the nanoparticle may be regarded as a special compatibilizer. Here, comparing with the conventional coil one, we define the nanoparticle (II of Figure 1) as a novel rigid compatibilizer. Earlier, Ginzburg[21] mentioned that the nanoparticles can be used as potential compatibilizers for mixtures of immiscible polymers. Hore and Laradji[22] also defined the nanorods as an emulsifying agent of immiscible blends. However, up to now, work on the quantitative relationship between the nanoparticles and the interfacial properties has been rare except for our previous work.[20] In fact, the relationship is very important to the studies on polymer blends and their interfaces, the self-assembly of nanoparticles, compatibilizers or emulsifiers, and so on.

Here, we study the effect of Janus nanorods [surface-modified by two different polymers, Figure 1(d)] on the interfacial properties of incompatible A/B homopolymer blends and emphasize the construction of a measurable relation between them. For this aim, a large parameter space must be considered. Accordingly, this would restrict the use of expensive experimental methods. It is lucky that the economical computer simulation methods have enough capability to provide valuable microscopic insights into the interfacial behaviors of the immiscible systems, especially with the dissipative particle dynamics (DPD) method. Specifically, Groot and Warren[23] first used DPD to calculate the interfacial tension of unlike polymers. Maiti and McGrother[24] showed a quantitative agreement between DPD-calculated interfacial tension and that from experiments for several liquid/liquid blends if a suitable coarse-graining process

was applied. Later, based on the general model, Qian *et al.*[25] utilized DPD to study the interfaces of incompatible A/B homopolymer blends in the presence of their block copolymers. Fan and Striolo[26] investigated the influence of nanoparticles on water/oil interfaces. Guo *et al.*[27] performed DPD to investigate the multiscale effects of compatibilizers on A/B/C ternary blends under shear flow and reproduced the experimental observations on such systems. Recently, based on the suitable coarse-graining model of real systems, Jing *et al.*[28] used DPD to study interfacial tension in the ternary Triton X-100/toluene/H_2O system. The results showed that the DPD-calculated interfacial tension is in good agreement with the experiment. Ginzburg *et al.*[9] used DPD and self-consistent field theory to study the interfacial tension of ternary oil/water/surfactant mixtures. They found that the two methods show a semiquantitative agreement among themselves and with experimental data. All these studies adequately testified that DPD is an intrinsically promising tool in the simulation of two phases with correctly defined interfaces. Therefore, in this work, we also use DPD to investigate the interface of incompatible A/B homopolymer blends in the presence of Janus nanorods and try to provide a measurable relationship between interfacial tension and Janus nanorods.

EXPERIMENTAL

The DPD method, originally developed by Hoogerbrugge and Koelman,[30] is a coarse-grained particle-based dynamics simulation technique. The motion of DPD particles is still governed by Newton's equation, $dr_i/dt = v_i$ and $dv_i/dt = f_i$, which are integrated by a modified velocity-Verlet algorithm.[23] For simplicity, the particle mass is set as 1, and the cutoff radius r_c is used as the unit of length. Therefore, the force f_i on a particle i can be expressed by

$$\boldsymbol{f}_i = \sum_{i \neq j} (\boldsymbol{F}_{ij}^{C} + \boldsymbol{F}_{ij}^{D} + \boldsymbol{F}_{ij}^{R}) \tag{1}$$

in which a conservative force, a dissipative force, and a random force are respectively equal to

$$\begin{aligned} \boldsymbol{F}_{ij}^{C} &= \alpha_{ij}(1 - r_{ij})\boldsymbol{e}_{ij} \\ \boldsymbol{F}_{ij}^{D} &= -\gamma w^{D}(r_{ij})(\boldsymbol{e}_{ij} \cdot \boldsymbol{V}_{ij})\boldsymbol{e}_{ij} \\ \boldsymbol{F}_{ij}^{R} &= \sigma w^{R}(r_{ij})\xi_{ij}\Delta t^{-0.5}\boldsymbol{e}_{ij} \end{aligned} \tag{2}$$

where α_{ij} is the repulsion parameter between i and j, which reflects the chemical characteristics of the interacting particles; and $\mathbf{r}_{ij} = \mathbf{r}_i - \mathbf{r}_j$, $r_{ij} = |\mathbf{r}_{ij}|$, $\mathbf{e}_{ij} = \mathbf{r}_{ij}/r_{ij}$, and $\mathbf{v}_{ij} = \mathbf{v}_i - \mathbf{v}_j$. The variable ζ_{ij} is a Gaussian random number with zero mean and unit variance, γ is the friction constant, and σ characterizes the noise strength. Friction and noise obey the relation $\sigma^2 = 2\gamma k_B T$, where k_B is the Boltzmann constant and T is the temperature. The weight functions w^D and w^R are coupled together to form a thermostat and have a certain relation $w^D = (w^R)^2$ in order to satisfy the fluctuation-dissipation theorem.[31] Here the simple form for $w^D = (w^R)^2 = (1 - r_{ij})^2$, $\sigma = 3$, and $\rho = 3r_c^3$ are used following Groot and Warren.[23]

In the initial configuration, the homopolymers *Am* and *Bn* are placed in the distinct halves of the simulation box. Janus nanorods are added into the blends near the interface. This artificial

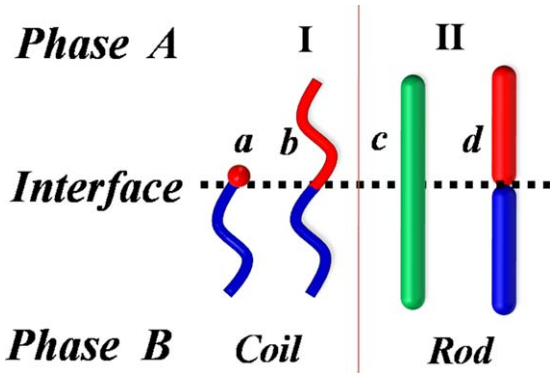

Figure 1. For I, the traditional coil compatibilizers including (a) the surfactants and (b) the block copolymers. For II, the novel rigid compatibilizers including (c) the homogenous nanorods and (d) the Janus nanorods. [Color figure can be viewed in the online issue, which is available at wileyonlinelibrary.com.]

behavior can speed up the formation of the interface and not influence the interfacial thermodynamics properties.[25] Janus nanorods are described by exerting the spring force F_{ij}^{S} and angle force F_{ij}^{A}, which are obtained by the differential of the spring and angle potential[20]:

$$\boldsymbol{F}_{(i,i+1)}^{S} = -\nabla U_{(i,i+1)}^{S};\ \ U_{(i,i+1)}^{S} = \sum_i \frac{1}{2} k_S \left(l_{(i,i+1)} - l_0\right)^2 \tag{3}$$

$$\begin{aligned} \boldsymbol{F}_{(i-1,i,i+1)}^{A} &= -\nabla U_{(i-1,i,i+1)}^{A};\ \ U_{(i-1,i,i+1)}^{A} \\ &= \sum_i k_A \left[1 - \cos\left(\varphi_{(i-1,i,i+1)} - \varphi_0\right)\right] \end{aligned} \tag{4}$$

where $l_{(i,i+1)}$ is the bond length between the connected two particles i and $i+1$, $\varphi_{(i-1,i,i+1)}$ is the bond angle of the adjacent three particles $i-1$, i, and $i+1$. Then, l_0 is fixed at 0.3 by a large spring coefficient $k_S = 40$, and $\varphi_0 = \pi$ is also fixed by a larger bending coefficient $k_A = 100$. The method describing nanorods is similar to that used by Chou *et al.*[32,33] The only difference is that the larger spring coefficients ($k_S = 100$) and a comparatively small bending constant ($k_A = 20$) are used in their works. Hence, the number density of nanorod particles is larger than that of the homopolymers *Am* and *Bn* ($k_S = 4$, $k_A = 0$), which can avoid undesired penetration of homopolymer particles into nanorods and overlap between nanorods.[34,35] The length of the Janus nanorod can be calculated by $L_{JR} = (x + y - 1) \times l_0$, which is a function of x and y. To ensure the accurate temperature control of the simulation system, the small integration steps $\Delta t = 0.01$ and 0.005 are used for the equilibrium progress and the result statistic, respectively.[36] Our simulation box is $40 \times 20 \times 20$ in size with periodic boundary conditions in the y and z directions. In the x direction, the wall is used to ensure only one interface, as shown in Figure 2(a). Figures 2(b) and 2(c) show the density distribution of every particle and the fluctuation of interfacial tension γ_S at the interface, respectively. Here, γ_S is calculated by $\gamma_S = \int [P_{xx} - 0.5(P_{yy} + P_{zz})]\,dx$, which is defined by the difference in normal and tangential stress across the interface. In simulations, the box was divided into 100 slabs parallel to the interface, and γ_S in each slab can be obtained by integrating the stress difference

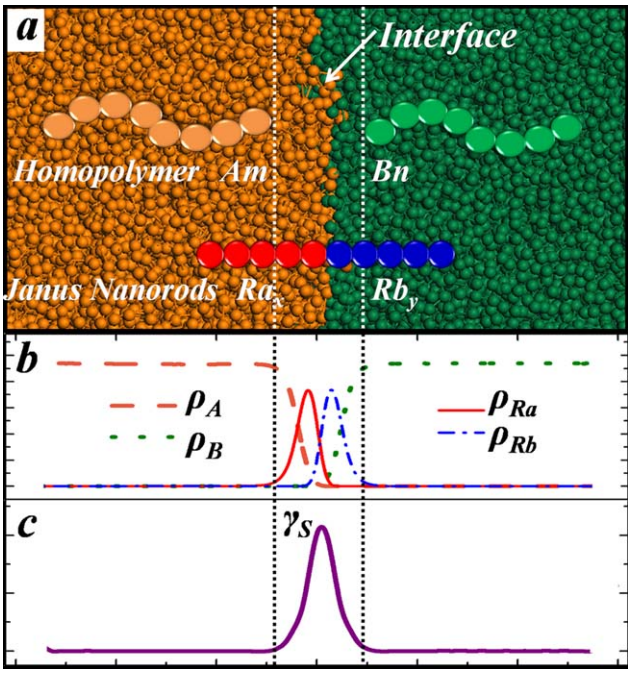

Figure 2. (a) The initial configuration of the blends including the coarse-grain models for homopolymers *Am* and *Bn* and Janus nanorods *Ra x Rb y*; (b) density profiles of the equilibrium system including homopolymers A and B and Janus nanorods; (c) interfacial tension profiles for the above system. [Color figure can be viewed in the online issue, which is available at wileyonlinelibrary.com.]

over *x*. For binary A/B blends, Qian *et al.*[25] had testified that a box of $20 \times 20 \times 20$ can avoid the finite size effect. For ternary A/B/nanorod mixtures, the longest $L_{JR} = 6.6$ for $x = 11$ and $y = 12$ is one-third of the shortest side of our box. Therefore, our box is also large enough to avoid the finite size effect according to the previous work.[20,25,34,35] By changing the other parameters, we systemically study the interface of incompatible A/B homopolymer blends in the presence of Janus nanorods. First, for the homopolymers, $m = n = 5$, 8, and 10 and $\alpha_{AB} = 30$, 40, 50, 60, and 80 are chosen to investigate the effect of chain length and the Flory-Huggins parameter χ (calculated by $\alpha_{ij} = 25 + 3.27\chi_{ij}$)[23] on the interface. Second, for symmetrical Janus nanorods with $x = y = 3$ and 7, α_{RaRb}, α_{BRa}, or $\alpha_{ARb} =$ 30, 40, 50, 60 and 80 are investigated to consider the effect of Janus nanorods with the different surface modifications on the interfacial tension. Third, unsymmetrical Janus nanorods are investigated by controlling *x* and *y*. Finally, the different volume ratios of Janus nanorods are studied.

RESULTS AND DISCUSSION

A/B Homopolymer Blends

The effects of the interaction parameter α_{AB} (or χ_{AB}) and the homopolymer chain length *m* (or *n*) on the interfacial tension γ_S were investigated, and the results are given in Figure 3. First, for the fixed chain length ($m = n = 5$, 8, and 10), the interfacial tension γ_S increases rapidly when increasing the repulsion parameter α_{AB} from 30 to 80 (χ_{AB} from 1.53 to 16.8). Second, from Figure 3 we can find that the increase of chain length (*m* or *n*) from 5 to 10 induces a minor increase in γ_S. The corresponding tendency from our simulations is in good agreement with the other work.[25,27] Therefore, we do not give more explanations in this part. Finally, we designated $\gamma_S = 0.31$ (at $\alpha_{AB} = 50$ and $m = n = 8$) as the reference value γ_{S^0} in the following context. The standard for improving the interfacial tension of immiscible A/B homopolymer blends ($\alpha_{AB} = 50$) is that the added compatibilizer can effectively drop the interfacial tension γ_S and make it less than the reference value γ_{S^0}.

Symmetrical Janus Nanorods (JRs)

If the JRs [represented by particles *Ra* and *Rb*; see Figure 2(a)] are surface-modified by the different polymers, they would have different interactions with the homopolymers. As a compatibilizer, we postulated two (*Ra* and *Rb*) parts are fully compatible with the homopolymers *Am* and *Bn*, respectively. This can be achieved by setting $\alpha_{ARa} = \alpha_{BRb} = 25$. In this way, we can place greater emphasis on investigating the effect of the repulsive parameters α_{RaRb} and α_{ARb} (or α_{Bra}) on the interfacial tension γ_S, except for the above fixed parameters $\alpha_{AB} = 50$ and $m = n = 8$. The volume ratio (ψ) of symmetric JRs is fixed at 0.03 for all blends. For convenience, the Janus nanorod is abbreviated as JR_{xy} in the following text, where *x* and *y* represent the number of *Ra* and *Rb*, respectively. For example, JR_{33} represents a symmetric Janus nanorod with $x = y = 3$. Figure 4 gives the relationship between γ_S and the two repulsive parameters (α_{RaRb} and α_{ARb}) for the two symmetric Janus nanorods JR_{33} and JR_{77}, respectively. To give a direct comparison with the traditional compatibilizer, Figures 4(c) and 4(d) also show the result on the relation between γ_S and the two repulsive parameters for coil–coil block copolymers (BPs). The coil–coil BPs (represented by *Ca* and *Cb*) are described by the same parameters as JRs, except for cancelling the restriction of rigidity (i.e., k_S is 4 not 40 and k_A is 0 not 100). For example, BP_{33} represents a symmetric coil–coil BP composed of three *Ca* beads and three *Cb* beads.

In Figure 4(a), with the increase of the repulsive parameter α_{RaRb}, JR_{33} and JR_{77} have a similar influence on the interfacial tension γ_S, which is that the increase of α_{RaRb} can make γ_S

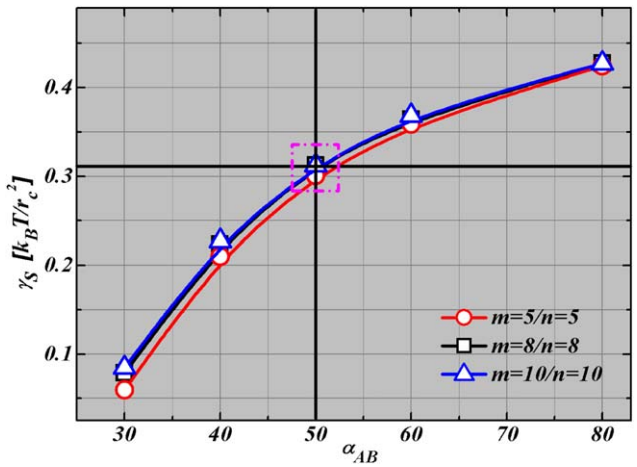

Figure 3. Interfacial tension γ_S as a function of the repulsive parameter α_{AB} for incompatible A/B homopolymer blends. [Color figure can be viewed in the online issue, which is available at wileyonlinelibrary.com.]

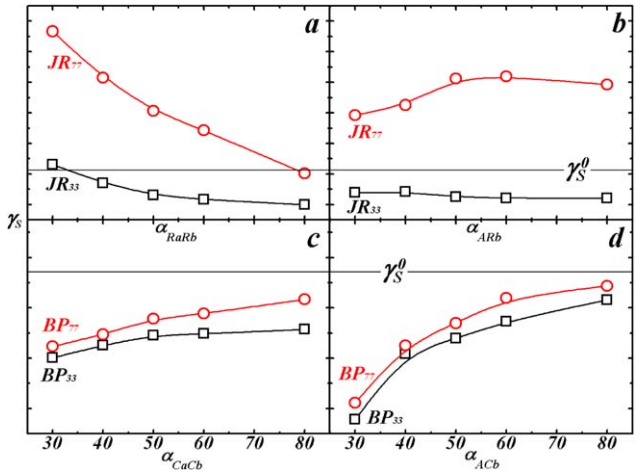

Figure 4. The interfacial tension γ_S of A/B blends with the rigid JR_{33}, JR_{77} and the coil BP_{33}, BP_{77} as a function of the repulsive parameters (a) α_{RaRb}, (b) α_{ARb}, (c) α_{CaCb}, and (d) α_{ACb}, respectively. [Color figure can be viewed in the online issue, which is available at wileyonlinelibrary.com.]

drop rapidly. However, with the increase of α_{ARb}, they have the different results that JR_{33} induces a slight decrease of γ_S and JR_{77} leads to a small increase in γ_S after $\alpha_{ARb} > 40$ [see Figure 4(b)]. It is a pity that, in comparing with the reference value γ_{S^0}, only JR_{33} can effectively decrease the interfacial tension, whereas the addition of JR_{77} can increase γ_S of A/B homopolymer blends and make them more than γ_{S^0}, which implies that the longer Janus nanorods are not a good compatibilizer. Under the identical parameters, the JRs are fully replaced by BPs; the interfacial tension γ_S of A/B blends in the presence of BPs are all less than γ_{S^0}, as shown in Figure 4(c,d). The difference is that γ_S gradually increases with increasing the parameters α_{CaCb} and α_{ACb}. As shown in Figure 4, it clearly shows that the longer BP_{77} is a better compatibilizer than JR_{77}, but we cannot further estimate the difference between BP_{33} and JR_{33} in reducing γ_S. Therefore, a single comparison for BP_{33} and JR_{33} is drawn in Figure 5. It is obvious that the γ_S of A/B blends using JR_{33} as a compatibilizer is more than that using BP_{33} in the range of small repulsive parameters α_{ARb} (α_{ACb}) < 40 and α_{RaRb} (α_{CaCb}) < 45. However, with the increase of repulsive parameters, the γ_S of A/B blends using JR_{33} as a compatibilizer will be less than that using BP_{33} in a broader range of α_{ARb} (α_{ACb}) > 40 and α_{RaRb} (α_{CaCb}) > 45, which fully clarifies that the efficiency of JR_{33} in reducing γ_S is higher than BP_{33}. Moreover, the difference in interfacial tensions will become larger with the increase in the repulsive parameters. Evidently, we can conclude that, as a compatibilizer, the shorter JR_{33} is a better choice than BP_{33} when the larger repulsive parameters are used.

In our previous work,[2] we found that there were two abilities that determine the effects of coil compatiblizers on reducing γ_S: the penetrability into each homopolymer phase and the ability to assemble at the interface. They can also be called the orientation and surface density (the number of surfactants at the interface per area).[25] First, in Figure 4(c,d), the γ_S of the blend with longer BP_{77} is larger than that with shorter BP_{33}, which agrees well with the previous work.[25] The reason is that the longer BP at the fixed concentration has a lower surface density. In general, we hope that there is a uniform explanation for all compatibilizers for their efficiency in improving γ_S. Therefore, the above two abilities are also used to analyze the difference between JRs in improving the γ_S of the blends. In Figure 6(a), JR_{77} has a higher surface density close to the interface than does JR_{33}. According to the above rules for the coil compatibilizer, the γ_S of the blends with JR_{77} should be lower than that with JR_{33}. However, Figure 4(a) shows an opposite result. Consequently, the surface density rule from the traditional coil compatibilizers is inapplicable to the novel JRs. Secondly, a structure (JRs are artificially placed perpendicular to the interface of A/B blends) is designed to check the applicability of the orientation rule in the novel JRs. A conformation after 10^3 steps (II) and an equilibrium conformation after 10^6 steps (I) are given in Figure 6(b). Figure 6(c) shows the evolution of γ_S and the orientation of JR_{77} with the simulation time, where the orientation of JR_{77} is described by the average included angle $<\theta_i>$ between the interface and JR_{77}, and the angle is calculated by $S = <(3\cos^2\theta - 1)/2>$. From Figure 6(b) we can see that conformation I (corresponding to $\theta_1 \approx 90$) has a wider density distribution than conformation II (corresponding to $\theta_4 \approx 18$), which shows that each JR in conformation I has a better ability to penetrate deep into its respective homopolymer phase than that in conformation II. Combining with Figure 6(c), we can conclude that the longer JR_{77} can also effectively reduce the γ_S and indeed make it less than γ_{S^0} like the shorter JR_{33} only when the nanorods adopt an orientation perpendicular to the interface. At the same time, the results show that the orientation rule is equally applicable to the traditional coil compatibilizer and to novel rigid ones. However, if there is no introduction of additional forces, the "standing" JRs in the artificial structure would gradually lie down toward the interface with the evolution of simulation time, as shown in Figure 6(c). This is a natural phenomenon especially for the longer JRs, which has been explained by the competitive relation between the entropic and enthalpic effects in the simulation[19] and the experiment.[37] The

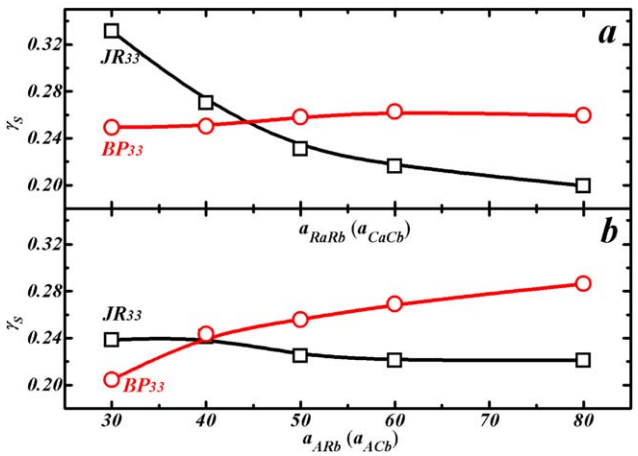

Figure 5. The interfacial tension γ_S of A/B blends with the rigid JR_{33} and the coil BP_{33} versus the repulsive parameters α_{RaRb} (α_{CaCb}) and α_{ARb} (α_{ACb}), respectively. [Color figure can be viewed in the online issue, which is available at wileyonlinelibrary.com.]

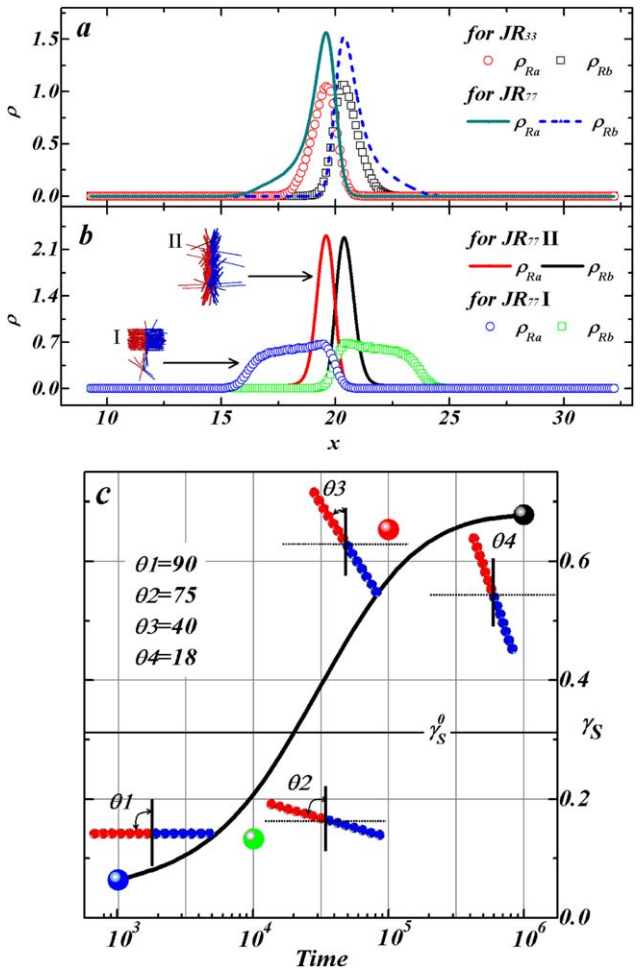

Figure 6. Density profiles near the interface for the particles (*Ra* and *Rb*) of Janus nanorods and the evolution of γ_S with the simulation time. (a) density profile for symmetric JR_{33} and JR_{77} with the same parameter space ($\alpha_{ARa} = \alpha_{BRb} = 25$, $\alpha_{ARb} = \alpha_{BRa} = \alpha_{RaRb} = 50$ and $\varphi = 0.03$); (b) density profile for symmetric JR_{77} (I); (c) the relationship between γ_S and θ_i (or time). [Color figure can be viewed in the online issue, which is available at wileyonlinelibrary.com.]

"lying" pose preferred by longer JRs would result in the increase of γ_S and make it larger than γ_{S^0}.

Unsymmetrical Janus Nanorods (*u*JRs)

If the ratio of the two homopolymers used in the surface modification by nanorods is not equal, it will result in the formation of unsymmetrical Janus nanorods (*u*JRs). Using the same parameters as before ($\alpha_{ARa} = \alpha_{BRb} = 25$, $\alpha_{ARb} = \alpha_{BRa} = \alpha_{RaRb} = 50$, and $\psi = 0.03$), three *u*JRs with fixed lengths ($x + y = 6$, 10, and 14) are used to investigate the effect of symmetric degree on γ_S. The changes in symmetric degree are achieved by varying the ratio of x/y. The result in Figure 7 clearly shows that the γ_S of the blends in the presence of *u*JRs will drop gradually with the reduction in the x/y value. When $x = 1$, the γ_S has a slight increase. However, it cannot influence the total tendency. Additionally, when the total length ($x + y$) of *u*JRs is more than 10, they cannot effectively improve the interfacial tension according to the criterion of $\gamma_S > \gamma_{S^0}$. Moreover,

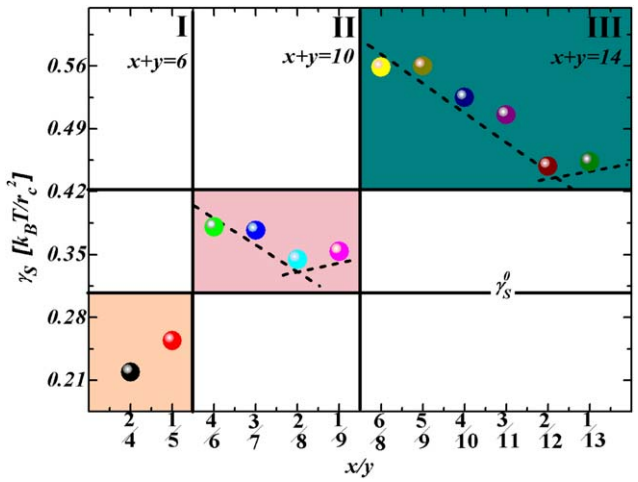

Figure 7. The relationship between the interfacial tension (γ_S) and the symmetric degree (x/y) for three *u*JRs with different lengths. [Color figure can be viewed in the online issue, which is available at wileyonlinelibrary.com.]

γ_S shows a stepped increase with the increase of *u*JR length ($x + y$). Thus, for example, the smallest γ_S for *u*JRs with $x + y = 14$ ($x/y = 2/12$) is still more than the largest one for *u*JRs with $x + y = 10$ ($x/y = 4/6$). Consequently, for both JRs and *u*JRs, the length is a decisive factor influencing the interfacial tension of the A/B homopolymer blends. This is a tight relation with the orientation rule.

Concentration of JRs (ψ)

In order to investigate the effects of concentration on γ_S, we do simulations at various concentrations of JRs with two lengths ($x = y = 3$ and 7). The concentration here denotes the volume fraction of JRs in the system. Figure 8 shows the variation of the interfacial tension (γ_S) with the increase of the JR concentration (ψ). It is interesting that there are two rules inverse to each other for the longer JR_{77} and the shorter JR_{33} in Figure 8. The interfacial tension γ_S decays monotonically as the concentration ψ of the shorter JR_{33} increases, which is consistent with

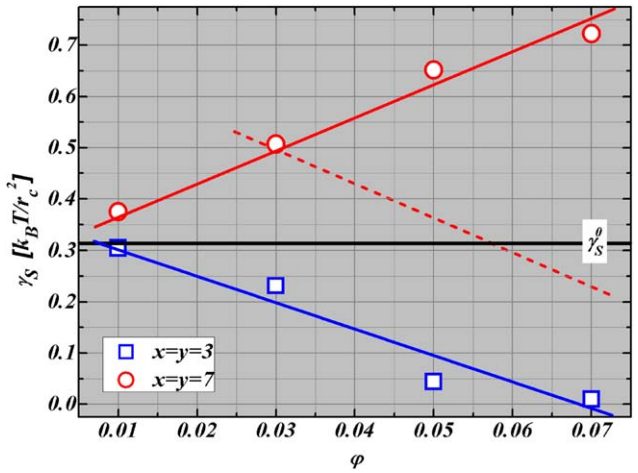

Figure 8. The relationship between the interfacial tension (γ_S) and the JRs concentration (φ) for JR_{33} and JR_{77}. [Color figure can be viewed in the online issue, which is available at wileyonlinelibrary.com.]

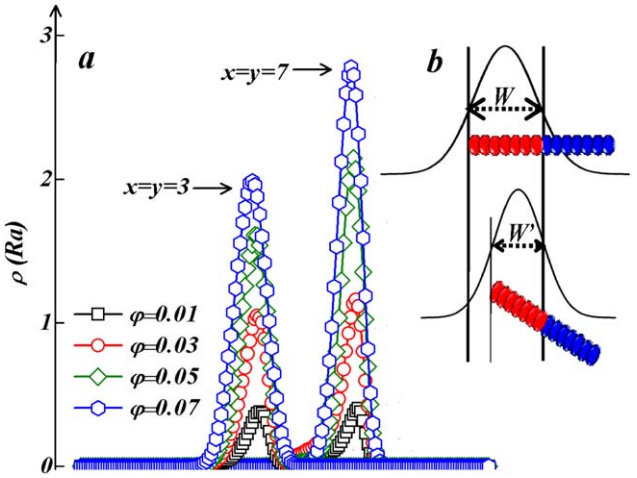

Figure 9. Density profiles for the particle *Ra* of JR_{33} and JR_{77} at various concentrations (a) and the schematic diagram of the Gaussian fitting (b). [Color figure can be viewed in the online issue, which is available at wileyonlinelibrary.com.]

the coil compatibilizer.[2,25,38] As a compatibilizer, this is a good behavior because we can easily control the interfacial tension of A/B homopolymer blends by tuning the concentration of compatibilizers. In fact, we hope the longer JR_{77} would have a functional relationship similar to the dashed line drawn in Figure 8. In that case, we can still use the longer Janus nanorods as a compatibilizer by increasing their content, although they always make $\gamma_S > \gamma_{S^0}$ at low concentrations. However, the longer JR_{77} makes γ_S rise monotonically with an increase in the concentration. This is not a good behavior for a compatibilizer.

In order to investigate the different behavior of JRs, we can still get an insight into this question from the angle of orientation. Figure 9(a) gives the density distribution of the bead *Ra* in JR_{33} and JR_{77} at various concentrations. From these results we can clearly see the growth of surface density with the increase of ψ. However, we cannot distinguish the breadth of the density distribution. As mentioned above, the surface density rule is inapplicable to JRs. Because of the normal distribution of $\rho(Ra)$, we fitted the density curves with a Gaussian function and calculated the half-height width (W) of the Gaussian function, as shown in Figure 9(b). We can see that, for the same JRs, the larger W corresponds to the "standing" JR [or the larger θ_i as shown in Figure 6(c)], and the smaller W' corresponds to the "lying" one (the small θ_i). Simultaneously, the "standing" pose of JR also denotes stronger penetrability than the "lying" pose. Thus, we can use the half-height width (W) of the Gaussian function to describe the orientation of JRs (or the penetrability into each homopolymer phase) and further explain the variation of γ_S. All the calculated W_{33} (for JR_{33}) and W_{77} (for JR_{77}) values at various concentrations are listed in Table I. From the data in Table I, we can find that W_{33} (for JR_{33}) has an obvious increase and W_{77} (for JR_{77}) has a slight decline as the concentrations increase. The increase of W_{33}, which denotes the increase of θ_i, will result in high efficiency in reducing γ_S and the lower interfacial tension γ_S. The decline of W_{77} implies that JR_{77} will induce an increase in γ_S. These results are in good agreement with those in Figure 8. Furthermore, we compare the two values of W_{33} and W_{77} at $\psi = 0.03$, and the result is $W_{33} > W_{77}$. Because of the same volume fraction, there are the same numbers of *Ra* and *Rb* for all JRs with different lengths. JRs with the longer length should have the broader density distribution (which indicates the larger W value) if they are perpendicular to the interface or have the same θ_i. In fact, JR_{77} has a narrower distribution than JR_{33} ($W_{77} < W_{33}$), which implies that the two amphiphilic segments of JR_{33} penetrate deeper into its respective homopolymer phase than those of JR_{77}. The corresponding results are that JR_{33} can effectively reduce the interfacial tension and, inversely, JR_{77} can increase γ_S, as shown in Figure 4(a). By combining these two results, the viewpoint that the orientation is a crucial factor that decides the ability of JRs to improve the γ_S of the A/B homopolymer blends is evidenced again.

Table I. The Half-Height Widths W_{33} (for JR_{33}) and W_{77} (for JR_{77}) at Various Concentrations

	ψ			
Width	0.01	0.03	0.05	0.07
W_{33}	0.95	1.05	1.16	1.29
W_{77}	0.92	0.91	0.88	0.85

CONCLUSIONS

In summary, Janus nanorods from the appropriate surface chemical modification are first used as a novel rigid compatibilizer to improve the interfacial tension of immiscible A/B homopolymer blend systems. Based on DPD simulations, the influence of the different Janus nanorods on the interfacial tension is systemically investigated. Compared with the traditional coil compatibilizer, the novel JRs can also improve the interfacial tension of homopolymer blends effectively; however, the optimal parameters have to be chosen.

For the traditional coil compatibilizer, there are two abilities that decide their efficiency in improving the interfacial tension. They are the ability to penetrate into each homopolymer phase and the ability to assemble at the interface, described by the orientation and surface density. However, only the orientation rule is applicable to the novel rigid compatibilizer (JRs). Specifically, the ability of JRs to reduce γ_S will become stronger with the increase of the angle θ_i between the interface and JRs. For example, the shorter JRs, which generally prefer the "standing" pose, can effectively penetrate deeper into the homopolymer phase. This can make them effectively decrease the γ_S and obtain the smallest γ_S value. Inversely, the longer JRs prefer the "lying" pose. Therefore, the absence of the ability to penetrate into the homopolymer phase results in the larger γ_S value and, sometimes, can let γ_S be more than the reference value γ_{S^0}. In other words, the shorter JRs (such as JR_{33} in this work) are a better compatibilizer than the longer ones and the corresponding coil compatibilizer. If the longer JRs can be controlled by the additional forces and adopt an orientation perpendicular to the interface, they are also a good choice as a compatibilizer.

Generally, polymer blends are used as a scaffold for tuning the novel electronic, optical, biomedical, and magnetic properties of nanoparticles. This simulation work can widen the application of nanoparticles. Taking nanorods as an example, a homogenous nanorod or the amphiphilic Janus nanorod can be used as a novel rigid compatibilizer to improve the interfacial properties and, at the same time, preserve their physical and chemical properties.

ACKNOWLEDGMENTS

The authors acknowledge the support of the Foundation of CAEP (No. 2014B0302040, 2014-1-075) and the National Nature Sciences Foundation of China (No. 11402241). The computation resources in the Simulation Center of CAEP are appreciated.

REFERENCES

1. Paul, D. R.; Bucknall, C. B. Polymer Blends: Formulation; Wiley: New York, **2000**.
2. Zhou, Y.; Long, X.-P.; Zeng, Q.-X. J. *Appl. Polym. Sci.* **2012**, *125*, 1530.
3. Kim, K. H.; Jo, W. H. *Macromolecules* **2007**, *40*, 3708.
4. Li, Y.; Shimizu, H. *ACS Appl. Mater. Interfaces* **2009**, *1*, 1650.
5. Shi, L.; Tummala, N. R.; Striolo, A. *Langmuir* **2010**, *26*, 5462.
6. Bagheri-Kazemabad, S.; Fox, D.; Chen, Y.; Geever, L. M.; Khavandi, A.; Bagheri, R.; Higginbotham, C. L.; Zhang, H.; Chen, B. *Compos. Sci. Technol.* **2012**, *72*, 1697.
7. Xu, Y.; Thurber, C. M.; Lodge, T. P.; Hillmyer, M. A. *Macromolecules* **2012**, *45*, 9604.
8. Malik, R.; Hall, C. K.; Genzer, J. *Soft Matter* **2011**, *7*, 10620.
9. Lin, Y.; Boker, A.; He, J.; Sill, K.; Xiang, H.; Abetz, C.; Li, X.; Wang, J.; Emrick, T.; Long, S.; Wang, Q.; Balazs, A.; Russell, T. P. *Nature* **2005**, *434*, 55.
10. Sun, B.; Sirringhaus, H. J. *Am. Chem. Soc.* **2006**, *128*, 16231.
11. Kim, B. J.; Fredrickson, G. H.; Hawker, C. J.; Kramer, E. J. *Langmuir* **2007**, *23*, 7804.
12. Dai, L. L.; Sharma, R.; Wu, C.-Y. *Langmuir* **2005**, *21*, 2641.
13. Luo, M.; Mazyar, O. A.; Zhu, Q.; Vaughn, M. W.; Hase, W. L.; Dai, L. L. *Langmuir* **2006**, *22*, 6385.
14. Ma, H.; Luo, M.; Dai, L. L. *Phys. Chem. Chem. Phys.* **2008**, *10*, 2207.
15. Luo, M.; Song, Y.; Dai, L. L. *Mol. Simul.* **2009**, *35*, 773.
16. Fan, H.; Resasco, D. E.; Striolo, A. *Langmuir* **2011**, *27*, 5264.
17. Yan, L.-T.; Popp, N.; Ghosh, S.-K.; Böker, A. *ACS Nano* **2010**, *4*, 913.
18. Yan, L.-T.; Maresov, E.; Buxton, G. A.; Balazs, A. C. *Soft Matter* **2011**, *7*, 595.
19. Xu, K.; Guo, R.; Dong, B.; Yan, L.-T. *Soft Matter* **2012**, *8*, 9581.
20. Zhou, Y.; Long, X.-P.; Zeng, Q.-X. *Polymer* **2011**, *52*, 6110.
21. Ginzburg, V. V. *Macromolecules* **2005**, *38*, 2362.
22. Hore, M. J. A.; Laradji, M. J. *Chem. Phys.* **2008**, *128*, 054901.
23. Groot, R. D.; Warren, P. B. J. *Chem. Phys.* **1997**, *107*, 4423.
24. Maiti, A.; McGrother, S. J. *Chem. Phys.* **2004**, *120*, 1594.
25. Qian, H.-J.; Lu, Z.-Y.; Chen, L.-J.; Li, Z.-S.; Sun, C. J. *Chem. Phys.* **2005**, *122*, 184907.
26. Fan, H.; Striolo, A. *Phys. Rev. E* **2012**, *86*, 051610.
27. Guo, R.; Li, J.; Yan, L.-T.; Xie, X.-M. *Soft Matter* **2013**, *9*, 255.
28. Jing, B.; Zhang, J.; Lu, X.; Zhu, Y.-J.; Zhang, F.-J.; Jiang, W.; Tan, Y.-B. *Acta Phys.-Chim. Sin.* **2011**, *27*, 65.
29. Ginzburg, V. V.; Chang, K.; Jog, P. K.; Argenton, A. B.; Rakesh, L. J. *Phys. Chem. B* **2011**, *115*, 4654.
30. Hoogerbrugge, P. J. *Europhys. Lett.* **1992**, *19*, 155.
31. Español, P.; Warren, P. B. *Europhys. Lett.* **1995**, *30*, 191.
32. Chou, S.-H.; Tsao, H.-K.; Sheng, Y.-J. J. *Chem. Phys.* **2011**, *134*, 034904.
33. Chou, S.-H.; Wu, D. T.; Tsao, H.-K.; Sheng, Y.-J. *Soft Matter* **2011**, *7*, 9119.
34. He, L.; Zhang, L.; Liang, H. *Polymer* **2010**, *51*, 3303.
35. He, L.; Pan, Z.; Zhang, L.; Liang, H. *Soft Matter* **2011**, *7*, 1147.
36. Zhou, Y.; Long, X.-P.; Zeng, Q.-X. *Mol. Simul.* **2012**, *38*, 961.
37. Deshmukh, R. D.; Liu, Y.; Composto, R. J. *Nano Lett.* **2007**, *7*, 3662.
38. Kim, S. H.; Jo, W. H. J. *Chem. Phys.* **1999**, *110*, 12193.